Vertical cloud climatology during TC4 derived from high-altitude aircraft merged lidar and radar profiles

Dennis Hlavka, SSAI, Dennis.L.Hlavka@nasa.gov
Lin Tian, UMBC, lin.tian-1@nasa.gov
William Hart, SSAI, William.d.hart@nasa.gov
Lihua Li, GSFC, lihua.li-1@nasa.gov
Matthew McGill, GSFC, matthew.j.mcgill@nasa.gov
Gerald Heymsfield, GSFC, Gerald.m.heymsfield@nasa.gov

(June 2009) Submitted to Journal of Geophysical Research

Aircraft lidar works by shooting laser pulses toward the earth and recording the return time and intensity of any of the light returning to the aircraft after scattering off atmospheric particles and/or the Earth's surface. The scattered light signatures can be analyzed to tell the exact location of cloud and aerosol layers and, with the aid of a few optical assumptions, can be analyzed to retrieve estimates of optical properties such as atmospheric transparency. Radar works in a similar fashion except it sends pulses toward earth at a much larger wavelength than lidar. Radar records the return time and intensity of cloud or rain reflection returning to the aircraft. Lidar can measure scatter from optically thin cirrus and aerosol layers whose particles are too small for the radar to detect. Radar can provide reflection profiles through thick cloud layers of larger particles that lidar cannot penetrate. Only after merging the two instrument products can accurate measurements of the locations of all layers in the full atmospheric column be achieved. Accurate knowledge of the vertical distribution of clouds is important information for understanding the Earth/atmosphere radiative balance and for improving weather/climate forecast models.

This paper describes one such merged data set developed from the Tropical Composition, Cloud and Climate Coupling (TC4) experiment based in Costa Rica in July-August 2007 using the nadir viewing Cloud Physics Lidar (CPL) and the Cloud Radar System (CRS) on board the NASA ER-2 aircraft. Statistics were developed concerning cloud probability through the atmospheric column and frequency of the number of cloud layers. These statistics were calculated for the full study area, four sub-regions, and over land compared to over ocean across all available flights. The results are valid for the TC4 experiment only, as preferred cloud patterns took priority during mission planning.

The TC4 Study Area was a very cloudy region, with cloudy profiles occurring 94 percent of the time during the ER-2 flights. One to three cloud layers were common, with the average calculated at 2.03 layers per profile. The upper troposphere had a cloud frequency generally over 30%, reaching 42 percent near 13 km during the study. There were regional differences. The Caribbean was much clearer than the Pacific regions. Land had a much higher frequency of high clouds than ocean areas. One region just south and west of Panama had a high probability of clouds below 15 km altitude with the frequency never dropping below 25% and reaching a maximum of 60% at 11-13 km altitude. These cloud statistics will help characterize the cloud volume for TC4 scientists as they try to understand the complexities of the tropical atmosphere.

Vertical cloud climatology during TC4 derived from high-altitude aircraft merged lidar and radar profiles

Dennis L. Hlavka[1], Lin Tian[2], William D. Hart[1], Lihua Li[3], Matthew J. McGill[4], Gerald M. Heymsfield[4]

[1]Science Systems and Applications, Inc. at NASA Goddard Space Flight Center
[2]University of Maryland Baltimore County at NASA Goddard Space Flight Center
[3]Code 555, NASA Goddard Space Flight Center
[4]Code 613.1, Laboratory of Atmospheres, NASA Goddard Space Flight Center

ABSTRACT: Only in recent years when nadir pointing lidars and cloud-profiling radars flew together on high-altitude aircraft or satellites have accurate measurements of the locations of all cloud layers in the full atmospheric column been achievable. Lidar provides sensitivity to thin layers whose particles are too small for the radar to see; radar provides the beam penetration through thick cloud layers that lidar cannot penetrate.

NASA ER-2 aircraft experiments have provided the opportunity to formulate sets of vertical cloud location profiles using the Cloud Physics Lidar (CPL) and the Cloud Radar System (CRS). This paper focuses on results from the Tropical Composition, Cloud and Climate Coupling (TC4) campaign based in Costa Rica in July-August 2007.

The unique data set that was developed produces cloud location arrays along track for every flight. Profiles show where lidar only, radar only, or both are observed. Statistics of vertical cloud probability and average number of cloud layers are shown for the whole study area, sub-regions, and for land versus ocean areas. The percentages of cloudy pixels and of surface return detections are calculated.

Although the cloud patterns flown over with the ER-2 were biased toward specific experiment objectives, the merged data set provides an excellent tool for characterizing the vertical cloud distributions that were actually observed during the campaign. The

30 flights sampled an area where cloud occurrence was 94%. The upper troposphere had
31 a cloud frequency reaching 42% during the study. The Caribbean was the most cloud-
32 free while the Panama Bight was the cloudiest.
33
34 **1. Introduction**
35 Accurate knowledge of the vertical distribution of clouds is important information for
36 understanding the Earth/atmosphere radiative balance and for improving
37 weather/climate forecast models (McFarquhar et al., 2000). Nadir pointing lidar and
38 cloud radar profiles obtained from high-altitude aircraft or satellites are complementary
39 measurements and have only recently shown their utility for obtaining accurate
40 information on the locations of all cloud layers in the full atmospheric column (McGill et
41 al., 2004 and Mace et al., 2009). Backscatter lidar measures attenuated backscatter up
42 to an optical depth threshold (~3.0). It is highly sensitive to optically thin cirrus and
43 aerosol layers whose particles are often too small for the radar to detect. Radar
44 measures reflectivity and is highly sensitive to clouds composed of large ice crystals
45 and can easily penetrate dense convective cloud that lidar cannot. Knowledge of the
46 overlap region where both instruments detect cloud signals is important for retrieval
47 algorithms for ice particle size and other cloud properties that use both radar and lidar
48 measurements. Excellent references for using combined lidar and radar data for cloud
49 retrieval properties are Okamoto et al. (2003) and Tinel et al. (2005).
50 Combined lidar and radar products were investigated in the U.S. using ground-based
51 instruments (Clothiaux et al., 2000). They obtained useful information, but had
52 difficulties with insects in the boundary layer and low thick clouds obscuring high thin

53 clouds. The conclusion was that they could not guarantee accurate full column cloud
54 locations. The first test of combining high-altitude (20 km) nadir lidar and radar data
55 was achieved during the Cirrus Regional Study of Tropical Anvils and Cirrus Layers-
56 Florida Area Cirrus Experiment (CRYSTAL-FACE) in July 2002 (Jensen et al, 2004)
57 using Cloud Physics Lidar (CPL) (McGill et al. 2002, 2003) backscatter measurements
58 at 532 and 1064 nm and the Cloud Radar System (CRS) (Li et al., 2004 and Racette et
59 al., 2003) reflectivity measurements at 94 GHz onboard the NASA ER-2 aircraft (McGill
60 et al., 2004). This study analyzed anvil morphology and radar optical depth (OD)
61 sensitivity for specific case studies. McGill et al. (2004) also describes the basic steps
62 for co-aligning and combining the lidar and radar data sets.
63 With the launch of the CloudSat (Stephens et al., 2002) and CALIPSO (Winker et al.,
64 2003) satellites in April 2006, a combined data set using the CALIOP lidar and CPR
65 radar has been developed and is called the 2B-GEOPROF-LIDAR product (Mace et al.
66 2007). It is the first cloud profiled observation set with global coverage, from June 2006
67 until present. Applications of this combined product are detailed in Mace et al. (2009).
68 Three NASA ER-2 aircraft experiments during the summers of 2006 and 2007, with
69 the CPL and CRS on board, have provided the opportunity to formulate new sets of
70 high-quality merged vertical cloud location profiles. In this paper, we will show results of
71 a straightforward cloud statistical analysis applied for the first time to an entire field
72 experiment, the Tropical Composition, Cloud and Climate Coupling (TC4) campaign
73 based in Costa Rica in July-August 2007. The focus of TC4 was to characterize the
74 cloud and chemical composition of the tropical tropopause region by satellite and high-
75 altitude aircraft remote sensing and medium and high-altitude aircraft in-situ

76 measurements. TC4 cloud properties are examined in the current study since we are
77 interested in understanding the cloud layer structure in a variety of complex tropical
78 cloud formations during TC4.
79
80 **2. Merged Data Sets and Products**
81 Our approach to merging CPL and CRS is similar to McGill et al. (2004), except that
82 CRS data is mapped directly to the CPL 30 m vertical bin locations to facilitate
83 implementation of joint algorithms using radar and lidar measurements. CRS reflectivity
84 is measured at a horizontal resolution of 0.5 s (~100 m along track) and a vertical
85 resolution of 37.5 m. CPL retrieves cloud and aerosol backscatter and optical
86 properties products at 1 s (~200 m along-track) horizontal resolution and 30.0 m vertical
87 resolution. CPL standard products contain top and bottom heights of all layers sensed
88 by the lidar, developed using an adjustable threshold algorithm. We developed a similar
89 threshold technique using the CRS reflectivity profiles to develop top and bottom
90 heights of all radar layers sensed. The minimum detectable reflectivity is about -28 dBZ
91 for CRS at a range of 15 km from the ER-2. We did not attempt to correct for radar
92 attenuation for the merged data sets, so the top and bottom height of the radar layers
93 are subject to the sensitivity of the CRS radar. CPL minimum detectable backscatter is
94 ~4.0 x 10^{-7} $m^{-1}sr^{-1}$ at a range of 10 km. This sensitivity allows for identification of sub-
95 visible cirrus and all significant aerosol layers.
96 CRS and CPL merged data sets and products were developed for each flight line
97 during TC4. Cloud and aerosol layer location for the full atmospheric column for every
98 ~200 m (1 s) along track were calculated for periods when both the CPL and CRS were

operating. These profiles show where lidar only, radar only, or both signals were observed. The corresponding temperature and pressure profiles, matching the resolution of the combined system, were also recorded. Surface return information for both lidar and radar were recorded. Statistics of vertical cloud probability and average number of cloud layers were calculated and regional differences were tabulated. The same statistics were tabulated for data over land verses over ocean. Overall percentage of cloudy pixels and frequency of lidar and radar surface return detection were formulated. Extinction and cumulative OD profiles from the CPL-sensed portion of the cloud column were passed to the merge file output.

To better understand the parameters involved in the statistical analysis of clouds during TC4, CPL-CRS merge products are calculated from a short segment (108 km) of the August 8, 2007 flight over the Pacific Ocean (Figure 1). Figure 1a shows an image of lidar vertical profiles from the optically thick anvil cirrus. The fact that there are no surface returns visible in the image is the only clue that the cloud is physically thicker than the lidar portrays. The lidar does however detect the very thin tropopause cirrus on the right side of the image at 16 km. Figure 1b images the merged signals of lidar and radar combined. In this image, the full vertical extend of the true cloud volume is shown. To image both the lidar and radar signals together, each were normalized based on their respective typical signal ranges. Radar surface returns are not displayed on this image.

From the type characterization map in Figure 2a, the total number of layers and the layer top and bottom heights can be calculated per profile. In this example, there were no aerosol layers detected. Cloud pixels sensed only by lidar are shown in green, only

by radar in red, and where both instruments sensed cloud in yellow. The yellow region is referred to as the overlap region. The overlap region varies in physical thickness depending on the cloud properties of the profile. Vertical cloud frequency profiles can be accumulated when a tally is kept where pixels are populated with clouds. The thick black line at the bottom of the characterization map of Figure 2a marks the detected surface return location for the CRS radar. The radar signal penetrates to the earth's surface and produces a signal spike when it hits the earth, unless the signal is totally attenuated by moderate to heavy rain. Therefore, lack of a radar surface return can be used to locate significant rain regions. There was no surface return detected by the lidar in this example. The lidar attenuates much sooner than the radar, and in general, attenuates at an optical depth of ~3.

Cumulative optical depth is another product from the merge file, calculated in the area of the cloud where an extinction profile can be retrieved from the lidar data. Figure 2b shows the lidar region of the anvil cloud in Figure 2a with cumulative optical depth displayed. From an experiment-wide accumulation of these profiles, the average height of a specific optical depth can be calculated.

3. Vertical Cloud Climatology during TC4

Merge data sets were processed for 12 of the 13 flights during TC4. CRS hardware problems caused July 25 data to be missed. The ER-2 was based at San Jose, Costa Rica and executed flights in and around Central America, the Caribbean Sea, and the Pacific Ocean. Cloud statistics were developed for the following five geographic regions: Full TC4 Study Area, San Jose, Panama Bight, Caribbean, and Pacific South.

145 Figure 3 shows the location of these regions on a map of Central America. The regions
146 were selected by the authors based on target areas during the TC4 deployment. Over
147 land versus over ocean statistics were also compared. We use the word climatology
148 loosely in this study since the data base only covers a 26 day period during one year.
149 Further, it does not capture much diurnal effect, with most flights in the local morning.
150 The fact that the days and locations of aircraft flights coincided with predefined cloud
151 pattern goals created a bias toward specific cloud patterns in each region. However,
152 this data base does accurately reflect the actual cloud distribution that was present
153 below the ER-2 aircraft for the duration of the experiment, which was our goal.

154 **3.1 Vertical Cloud Statistics by Geographic Region**

155 Table 1 displays various cloud statistics calculated during TC4 for the entire area
156 and the four sub-regions. The probability of having a cloud in any 1 s profile is very high
157 in all regions except the Caribbean. The Caribbean had a much different cloud pattern
158 compared to the other regions with a tendency to have only one or two scattered high
159 layers (if any at all) and only a few cumuli. The Pacific South region tended to have
160 more low clouds, especially stratocumulus. The other regions had complex cloud
161 systems at many levels. Inferring from the lidar surface return frequency for the full TC4
162 study area, only about 31% of the profiles had total column optical depth below 3.0.
163 The Caribbean region was an exception with 97%. The radar surface return frequency
164 was very high, averaging 93.5% for the full TC4 study area. This infers the percentage
165 of profiles where moderate or heavy rain obscured the radar reached 6.5%. On
166 average for the full study area, the vertical cloud zone ranged from 12.3 km down to 4.0

167 km, or 8.3 km thick. The region with the highest average cloud tops was the San Jose
168 region, where tops averaged 15.1 km.

169 The cumulative optical depth heights should be interpreted as follows: starting at the
170 aircraft altitude, the lower the height to reach the specific optical depth level, the more
171 transparent the middle and upper portion of the troposphere is. If the height is near sea
172 level, this means the atmosphere did not fully reach the optical depth threshold. For the
173 full study area, the average height of optical depth 1.0 was 6.0 km and optical depth 3.0
174 was 4.3 km. The Caribbean region easily had the most transparent atmosphere. It
175 should be noted that the cumulative optical depth includes aerosol layers. Only in the
176 Caribbean region were aerosols (Saharan dust) prevalent. The number of merged
177 profiles analyzed for each region is tabulated in the legend of Figure 4. An overall total
178 of 135525 profiles were analyzed. We note that the Caribbean region had six times
179 fewer profiles than did the region-by-region average, mostly due to the fact only two
180 flights focused on the region and one of those had missing data.

181 The two most important statistics from this study are the frequency distribution of the
182 number of cloud layers in the total atmospheric column and the vertical distribution of
183 those clouds. Figure 4 shows the frequency distribution of the number of cloud layers
184 for the full study area and the four sub-regions. The Pacific South region was a region
185 of optically thin cirrus layers and frequent stratocumulus. The Panama Bight region was
186 a region of active thunderstorms and complex cloud formations. Most regions averaged
187 near two layers per profile, with less than a 6% occurrence of clear sky and less than
188 2% occurrence of 6 or more layers. The Caribbean and the Pacific South were the
189 exceptions, averaging 0.70 and 1.68 layers, respectively. The Caribbean region was

dominated by clear sky (57% occurrence). The Pacific South region layer distribution showed a peak in the one-layer category, which occurred over 40% of the time.

To get a feel for the average cloud volume, Figure 5 shows the vertical frequency distribution of cloudy pixels in the full TC4 study area. Figure 6 shows the same for the four sub-regions. Each plot has four distributions: 1) CPL sensed clouds only (blue), 2) clouds sensed by both instruments (yellow), 3) CRS sensed clouds only (red), and 4) total cloud volume from the merged CPL/CRS clouds (green). The blue, yellow, and red plots are mutually exclusive and sum up to the green plot. For the TC4 study area as a whole, the chance of cloud occurrence was highest (just above 40%) between 12 and 13 km. The vertical distribution is somewhat bimodal with another frequency peak near 1 km, probably due to scattered cumulus and stratocumulus. The CPL found few clouds between 9 and 2 km because of signal attenuation, but did pick up the low cumulus when the signal was not fully attenuated. The radar observed its highest cloud frequency between 8 and 10 km.

Cloud volumes for the four regions in Figure 6 each show unique characteristics. For the Pacific South region, the highest frequency of clouds (32%) occurred below 1 km, influenced by the predominance of stratocumulus. Two other lesser peaks occurred, one at 10 km and another at 15 km. For the Panama Bight region, clouds were frequent at all levels, with the highest frequency (60%) at 12-13 km. Because of lidar signal attenuation, the cloud distribution relied on the CRS radar below 8 km. The San Jose region was dominated by clouds above 11 km, reaching 75% occurrence at 14 km. The Caribbean region showed a bimodal distribution, but each peak cloud frequency was less than 25%.

3.2 Vertical Cloud Statistics by Surface Type

The TC4 cloud analysis was also performed separately for land versus ocean areas. Because water dominates the region and was the preferred destination during most flights, there were six times more profiles over water than over land. Table 2 shows the same parameters as Table 1, except separated by water and land regions. Because the CRS surface return height was the parameter used to determine land or water, profiles that did not have a radar surface return were not used and thus the true frequency was not available. Both land and ocean categories had a high frequency of cloudy profiles and similar lidar surface return frequency. In this data base, profiles over land recorded the highest average cloud top height, which was 3.1 km higher than over the ocean. Profiles over land reached an optical depth value of 1.0 sooner, but reached a value of 3.0 later than over the ocean.

Figure 7 displays the layer count frequency distribution for profiles over land and water. The analysis showed that profiles over land had more of a tendency for multiple cloud layers, with an average of 2.35 layers, as opposed to profiles over the ocean, which had an average of 1.95. The number of profiles in each category is displayed in the legend. Figure 8 shows the vertical frequency distribution differences between clouds over land and over water. Profiles over land had a very high frequency (75%) of cloud between 13 and 14 km, but dropped off significantly below that altitude. The vertical cloud distribution over the ocean region mimics the study area as a whole with a minimum of 14% at 4 km and peaking at 37% at 12 km.

4. Conclusion

The newly developed CPL lidar and CRS radar merged product is an excellent tool for doing vertical cloud analysis and has helped to characterize the vertical cloud distributions during the TC4 field experiment. The results are valid for this field experiment only, as preferred cloud patterns took priority during mission planning. The TC4 Study Area was a very cloudy region, with cloudy profiles occurring 94% of the time during the ER-2 flights. One to three cloud layers were common, with the average calculated at 2.03 layers per profile. The average top of the highest cloud layer reached 12.350 km. From the CPL lidar data, it was determined that the average height where the cumulative optical depth reached 1.0 was at 5.968 km and where the optical depth reached 3.0 was at 4.258 km. From analysis of the vertical cloud distribution, the upper troposphere had a cloud frequency generally over 30%, reaching 42% near 13 km during the study. There were regional differences. The Caribbean was more cloud-free than the other regions. Profiles over land had a much higher frequency of high clouds than over ocean areas. The Panama Bight region had the highest probability of clouds throughout the vertical column, with the frequency never dropping below 25% below 15 km altitude.

Work is nearing completion on an enhanced merged ER-2 instrument data set that will include the MODIS Airborne Simulator (MAS) radiometer and vertical Doppler radar velocity for more complex data analysis.

Acknowledgments. The Cloud Physics Lidar and Cloud Radar System are supported by NASA's Radiation Sciences Program (Hal Maring, Program Manager). Data shown was collected as part of the Tropical Composition, Cloud and Climate Coupling (TC4) experiment.

References

Clothiaux, E. E., T. P. Ackerman, G. G. Mace, K. P. Moran, R. T. Marchand, M. A. Miller, and B. E. Martner (2000), Objective determination of cloud heights and radar reflectivities using a combination of active remote sensors at the ARM CART sites, *J. Appl. Meteorol., 39*, 645-665.

Li, L., G. M. Heymsfield, P. E. Racette, L. Tian, and E. Zenker, (2004), A 94 GHz cloud radar system on a NASA High-altitude ER-2 aircraft, *J. Atmos. Ocean. Technol., 21,* 1378-1388.

Jensen, E., D. Starr, and O. B. Toon (2004), Mission investgates tropical cirrus clouds, *Eos Trans. AGU, 84*(5), 45, 50.

Mace, G., D. Vane, G. Stephens, and D. Reinke (2007), Level 2 radar-lidar GEOPROF product: Version 1.0 process description and interface control document, Jet Propulsion Laboratory, California Institute of Technology, http://cloudsat.cira.colostate.edu/ICD/2B-GEOPROF-LIDAR/2B-GEOPROF-LIDAR_PDICD_1.0.doc.

Mace G. G., Q. Zhang, M. Vaughn, R. Marchand, G. Stephens, C. Trepte and D. Winker, (2009), A description of Hydrometeor layer occurrence statistics derived from the first year of merged CloudSat and Calypso data, doi:10.10.129/2007DJD009755, in press.

McFarquhar, G. M., A. J. Heymsfield, J. Spinhirne, and W. Hart (2000), Thin and subvisual tropopause tropical cirrus: Observations and radiative impacts, *J. Atmos. Sci., 57*, 1841-1853.

McGill, M.J., D.L. Hlavka, W.D. Hart, J.D. Spinhirne, V.S. Scott, and B. Schmid (2002), The Cloud Physics Lidar: Instrument description and initial measurement results, *Applied Optics, 41*, pg. 3725-3734.

McGill, M. J., D. L. Hlavka, W. D. Hart, E. J. Welton, and J. R. Campbell (2003) , Airborne lidar measurements of aerosol optical properties during SAFARI-2000, *J. Geophys. Res.,108*(D13), 8493, doi:10.101029/2002JD002370.

McGill, M.J., L. Li, W.D. Hart, G.M. Heymsfield, D.L. Hlavka, P.E. Racette, L. Tian, M.A. Vaughan, and D.M. Winker (2004), Combined lidar-radar remote sensing: Initial results from CRYSTAL-FACE, *Journal of Geophysical Research, 109*, D07203, doi: 10.1029/2003JD004030.

Okamoto, H., S. Iwasaki, M. Yasui, H. Horie, H. Kuroiwa, and H. Kumagai (2003), An algorithm for retrieval of cloud microphysics using 95-GHz cloud radar and lidar, *J. Geophys. Res., 108*(D7), 4226, doi:10.1029/2001JD001225.

Racette, P. E., G. M. Heymsfield, L. Li, L. Tian, and E. Zenker (2003), The cloud radar system, in *Proceedings of the 31st AMS Conference on Radar Meteorology*, pp. 237-240, Am. Meteorol. Soc., Boston, Mass.

Stephens, G. L., et al. (2002), The CloudSat mission and the A-Train: A new dimension of space-based observations of clouds and precipitation, *Bull. Am. Meteorol. Soc., 83*, 1771-1790.

Tinel, C., J. Testud, J. Pelon, R. J. Hogan, A. Protat, J. Delanoe, and D. Bouniol (2005), The retrieval of ice-cloud properties from cloud radar and lidar synergy, *J. Appl. Meteorol., 44,* 860-875.

Winker, D. M., J. R. Pelon, and M. P. McCormick (2003), The CALIPSO mission: Spaceborne lidar for observation of aerosols and clouds, in Lidar Remote Sensing for Industry and Environment Monitoring III, edited by U. Singh, T. Itabe, and Z. Liu, Proc. SPIE Int. Soc. Opt. Eng., 4893, 1–11.

317 **Table 1:** Cloud and Optical Statistics by Geographic Region

Statistic	Full TC4 Study Area	San Jose Region	Panama Bight Region	Caribbean Region	Pacific South Region
Cloudy Profile Frequency (%)	94.3	98.7	98.4	44.1	94.4
CPL Lidar Surface Return Frequency (%)	30.6	37.8	20.3	97.1	30.1
CRS Radar Surface Return Frequency (%)	93.5	89.6	91.2	99.9	99.3
Avg. Ht. (km) of Highest Cloud Top	12.350 (258.4 hPa)	15.087 (144.5 hPa)	13.364 (192.1 hPa)	10.704 (339.0 hPa)	8.709 (460.5 hPa)
Avg. Ht. (km) of Lowest Cloud Bottom	3.994 (700.2 hPa)	5.480 (607.3 hPa)	4.094 (680.5 hPa)	7.338 (516.8 hPa)	2.411 (826.9 hPa)
Avg. Ht. (km) where Cumulative OD Reaches 1.0	5.968 (590.6 hPa)	7.117 (537.3 hPa)	8.044 (453.1 hPa)	0.098 (1002.5 hPa)	2.103 (833.1 hPa)
Avg. Ht. (km) where Cumulative OD Reaches 3.0	4.258 (698.9 hPa)	3.457 (756.6 hPa)	6.470 (552.5 hPa)	0.085 (1003.9 hPa)	1.644 (866.9 hPa)

318
319
320

Table 2: Cloud and Optical Statistics by Surface Type

Statistic	Over Land	Over Ocean
Cloudy Profile Frequency (%)	96.2	93.6
CPL Lidar Surface Return Frequency (%)	39.8	31.0
Avg. Ht. (km) of Highest Cloud Top	14.870 (147.7 hPa)	11.733 (286.3 hPa)
Avg. Ht. (km) of Lowest Cloud Bottom	4.793 (646.1 hPa)	4.018 (700.7 hPa)
Avg. Ht. (km) where Cumulative OD Reaches 1.0	6.283 (567.5 hPa)	5.502 (619.0 hPa)
Avg. Ht. (km) where Cumulative OD Reaches 3.0	3.037 (762.3 hPa)	3.956 (719.3 hPa)

321

Figure Captions

Figure 1. a) CPL attenuated lidar profiles only and b) merged CPL lidar-CRS radar profiles during a nine minute (108 km) segment of the August 8, 2007 ER-2 flight over the Pacific Ocean during TC4. The fact that there are no lidar surface returns visible in (a) is the only clue that the cloud is physically thicker than the lidar portrays. In image (b), the full vertical extend of the true cloud volume is retrieved.

Figure 2. a) The type characterization map for the same scene as in Figure 1b. This maps the vertical location of cloud pixels that only CPL detected (green), cloud pixels that only CRS detected (red), and cloud pixels that were detected by both instruments (yellow). No aerosol layers were detected. The thick black line at 0 altitude is the radar surface return location indicator. b) Cumulative optical depth calculations from the CPL lidar portion of the cloud complex. In this case, the lidar signal becomes totally attenuated at an optical depth of ~3.0.

Figure 3. Map of the overall TC4 experiment study area (black box) and the four sub-regions of the experiment conducted July-August, 2007 near Central America. The San Jose region is green, the Caribbean region is yellow, the Panama Bight region is red, and the Pacific South region is blue.

Figure 4. The frequency distribution of the total number of cloud layers in the atmospheric column for the full TC4 experiment and each of the four sub-regions. The average number of cloud layers for the full study area was 2.03. Each sub-region showed a similar distribution except for the Caribbean region, which was much clearer. The number of profiles in each data set is shown in the legend.

Figure 5. The vertical cloud distribution statistics for the full TC4 experiment in 2007. CPL sensed clouds only are shown in blue, clouds sensed by both instruments are in yellow, CRS sensed clouds only are in red, and total cloud volume from the merged CPL/CRS clouds is in green. The blue, yellow, and red plots are mutually exclusive and sum up to the green plot.

Figure 6. The vertical cloud distribution statistics for the four sub-regions of the TC4 experiment of 2007. The plots are the same type as Figure 5. Each sub-region had its own unique distribution.

Figure 7. The frequency distribution of the total number of cloud layers over land (black) and over ocean (red). The average number of cloud layers for each region was 2.35 and 1.95 respectively. The number of profiles in each data set is shown in the legend.

Figure 8. The vertical cloud distribution statistics over land (left) and over ocean (right) for the TC4 experiment. CPL sensed clouds only are shown in blue, clouds sensed by both instruments are in yellow, CRS sensed clouds only are in red, and total cloud volume from the merged CPL/CRS clouds is in green. Land profiles, which occurred much less frequently than water profiles, contained high-altitude clouds over 70% of the time.

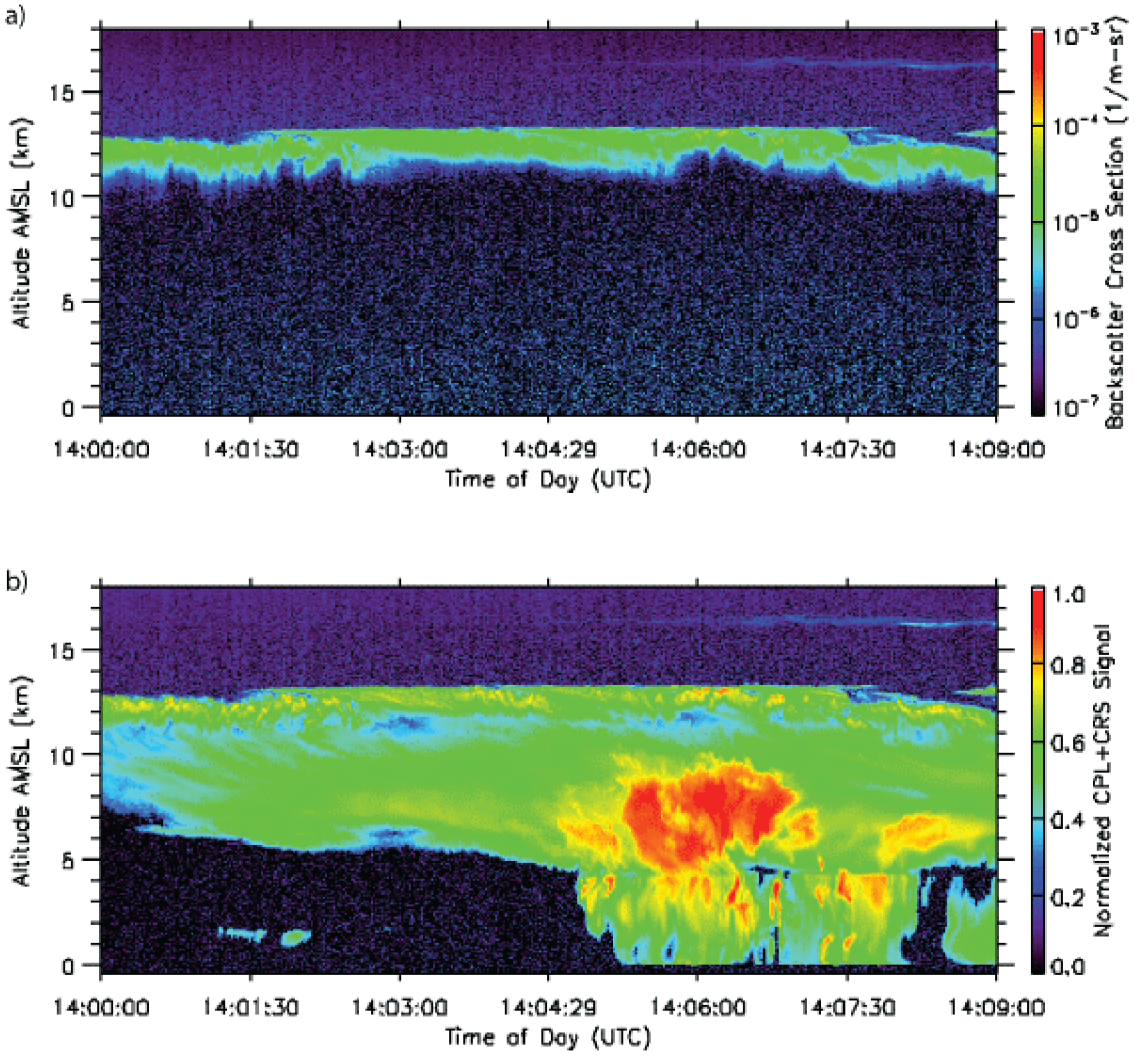

Figure 1. a) CPL attenuated lidar profiles only and b) merged CPL lidar-CRS radar profiles during a nine minute (108 km) segment of the August 8, 2007 ER-2 flight over the Pacific Ocean during TC4. The fact that there are no lidar surface returns visible in (a) is the only clue that the cloud is physically thicker than the lidar portrays. In image (b), the full vertical extend of the true cloud volume is retrieved.

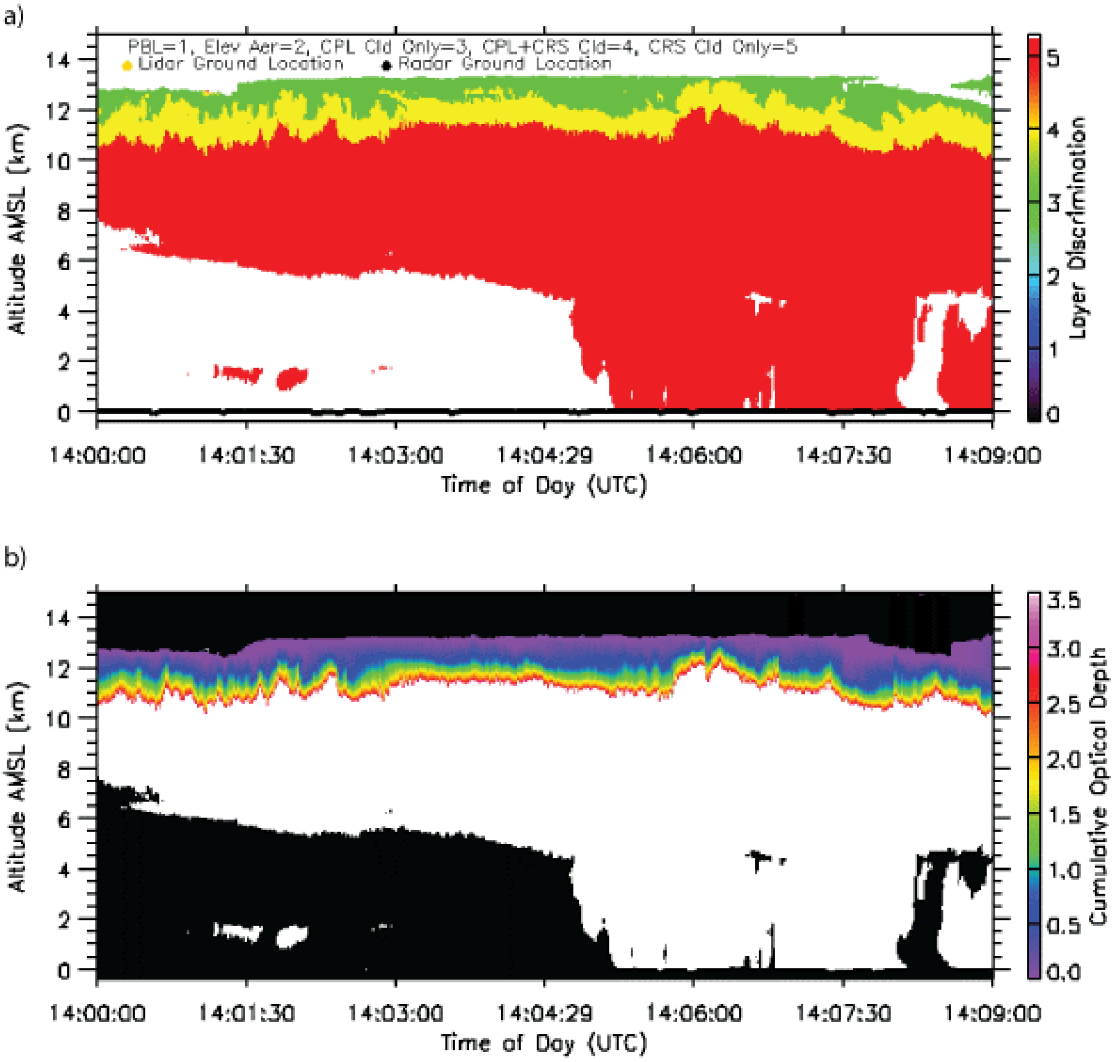

Figure 2. a) The type characterization map for the same scene as in Figure 1b. This maps the vertical location of cloud pixels that only CPL detected (green), cloud pixels that only CRS detected (red), and cloud pixels that were detected by both instruments (yellow). No aerosol layers were detected. The thick black line at 0 altitude is the radar surface return location indicator. b) Cumulative optical depth calculations from the CPL lidar portion of the cloud complex. In this case, the lidar signal becomes totally attenuated at an optical depth of ~3.0.

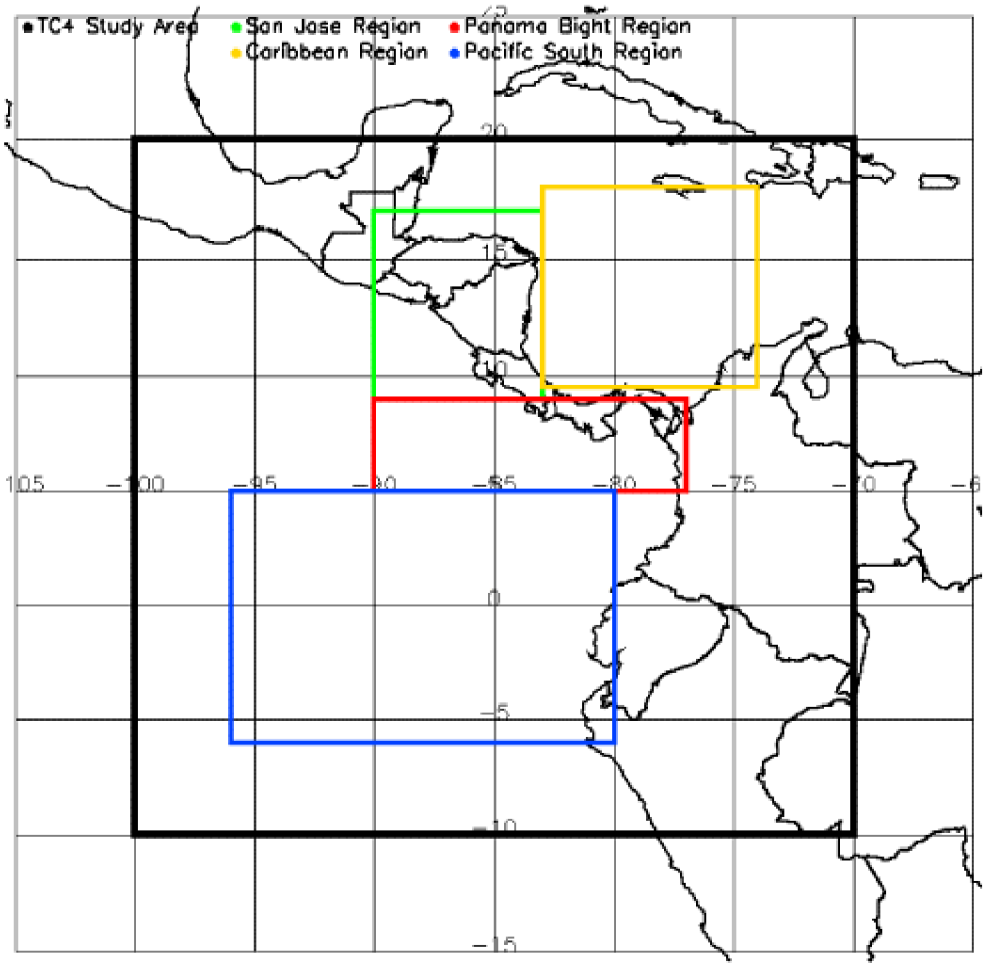

Figure 3. Map of the overall TC4 experiment study area (black box) and the four sub-regions of the experiment conducted July-August, 2007 near Central America. The San Jose region is green, the Caribbean region is yellow, the Panama Bight region is red, and the Pacific South region is blue.

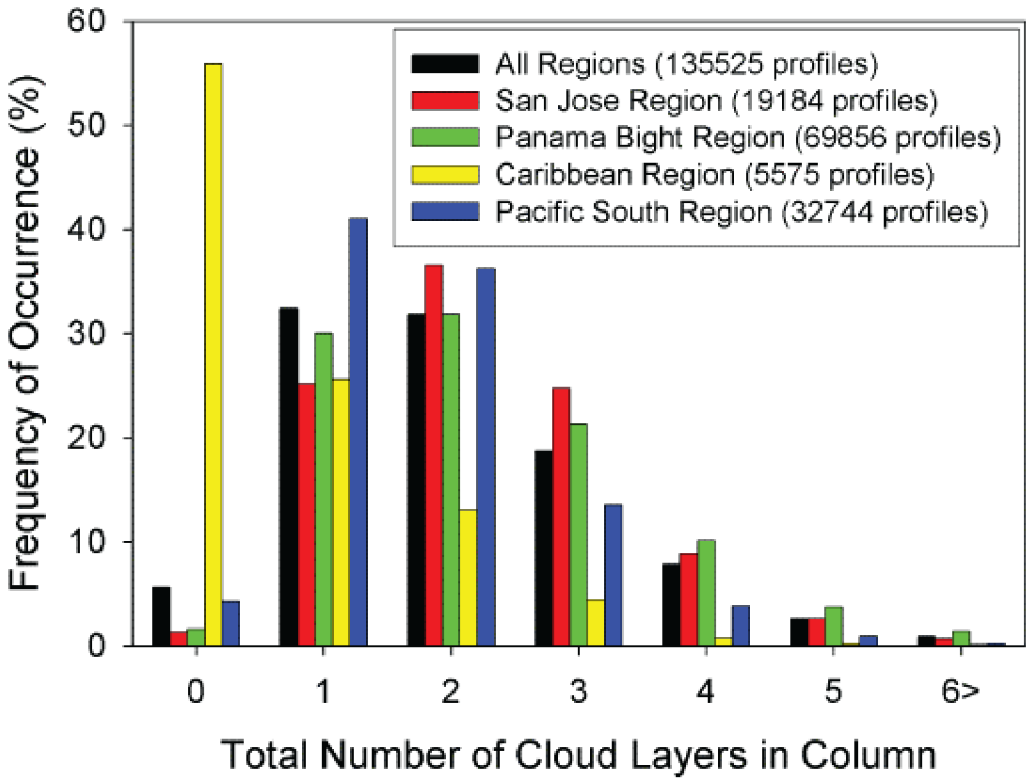

Figure 4. The frequency distribution of the total number of cloud layers in the atmospheric column for the full TC4 experiment and each of the four sub-regions. The average number of cloud layers for the full study area was 2.03. Each sub-region showed a similar distribution except for the Caribbean region, which was much clearer. The number of profiles in each data set is shown in the legend.

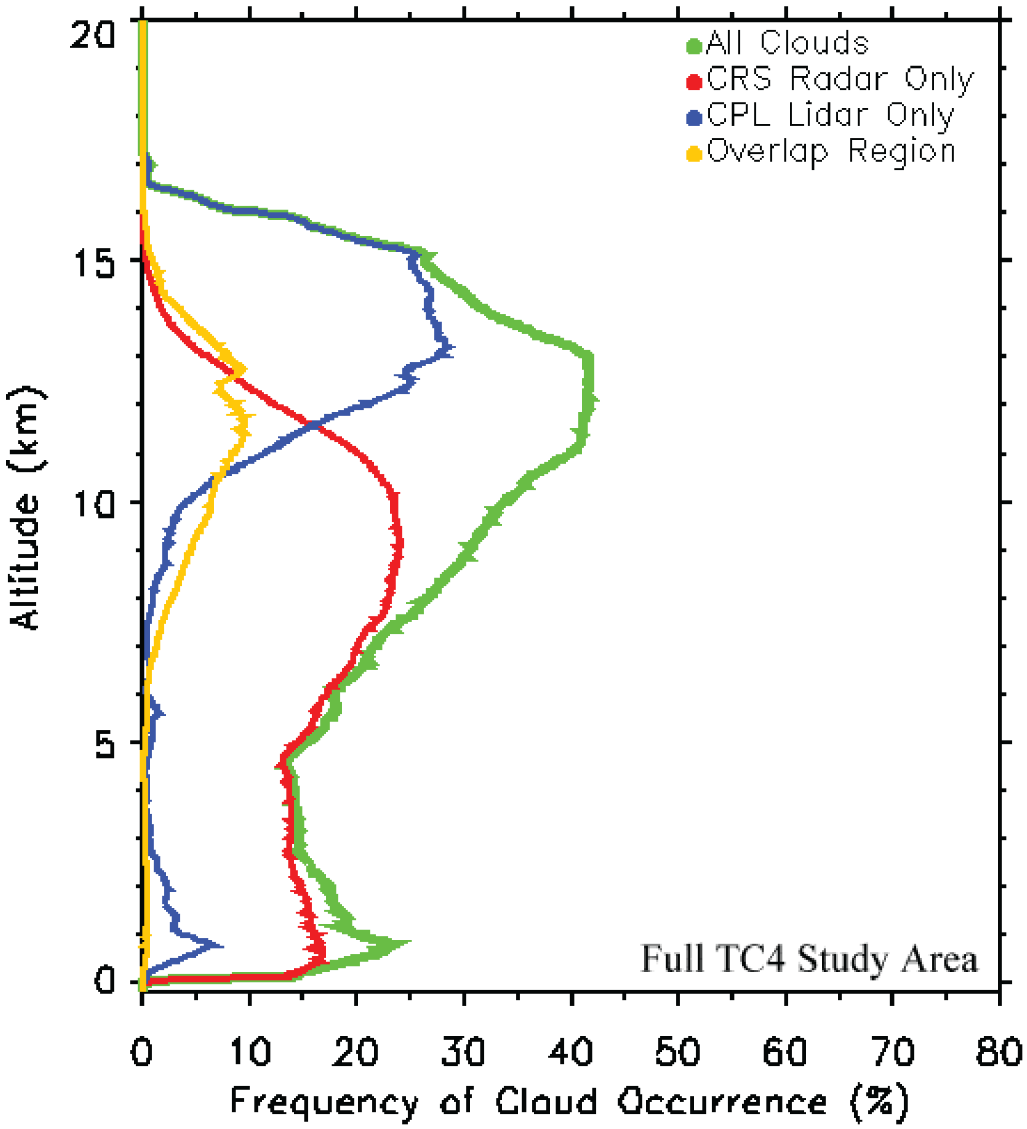

Figure 5. The vertical cloud distribution statistics for the full TC4 experiment in 2007. CPL sensed clouds only are shown in blue, clouds sensed by both instruments are in yellow, CRS sensed clouds only are in red, and total cloud volume from the merged CPL/CRS clouds is in green. The blue, yellow, and red plots are mutually exclusive and sum up to the green plot.

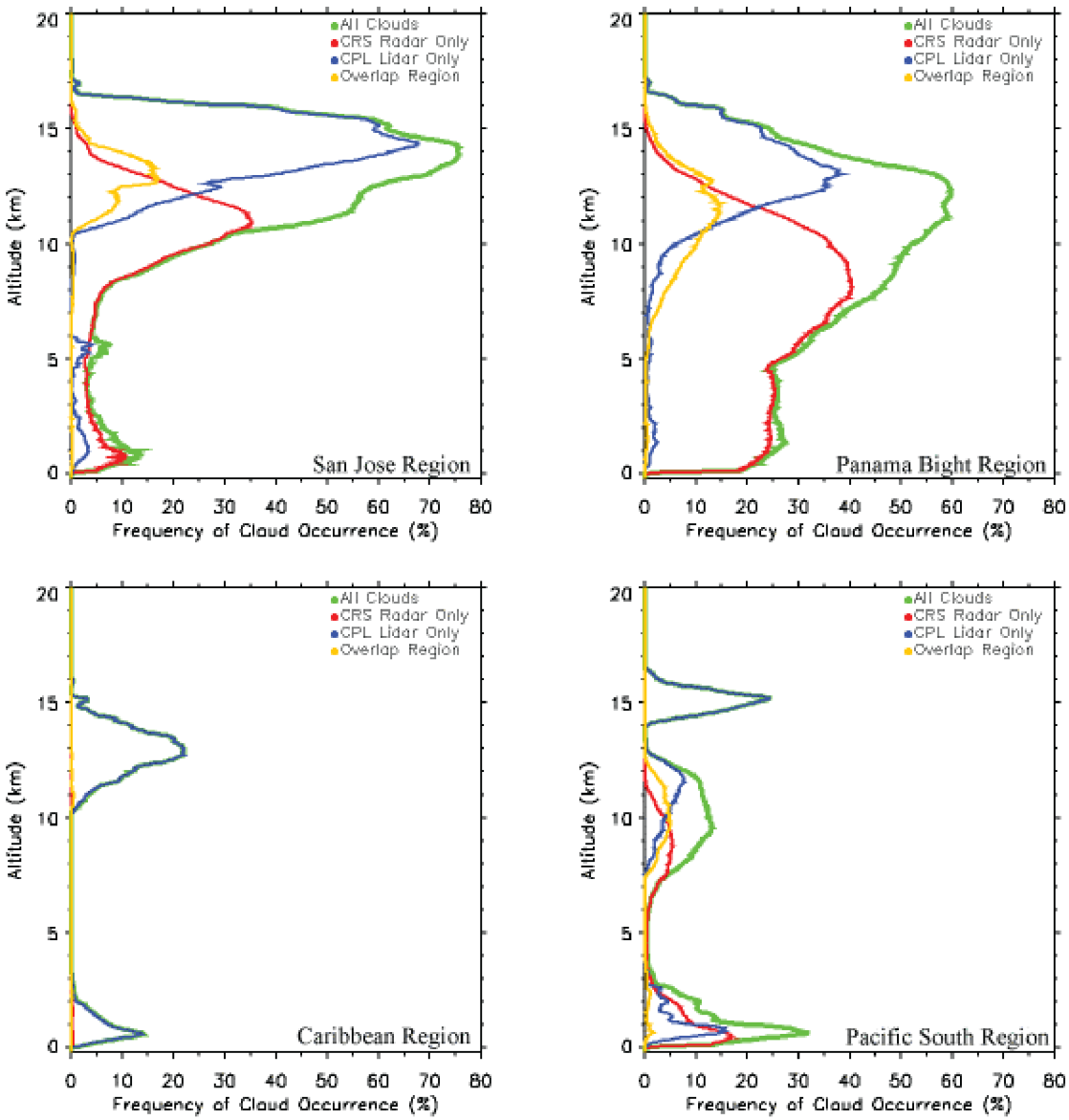

Figure 6. The vertical cloud distribution statistics for the four sub-regions of the TC4 experiment of 2007. The plots are the same type as Figure 5. Each sub-region had its own unique distribution.

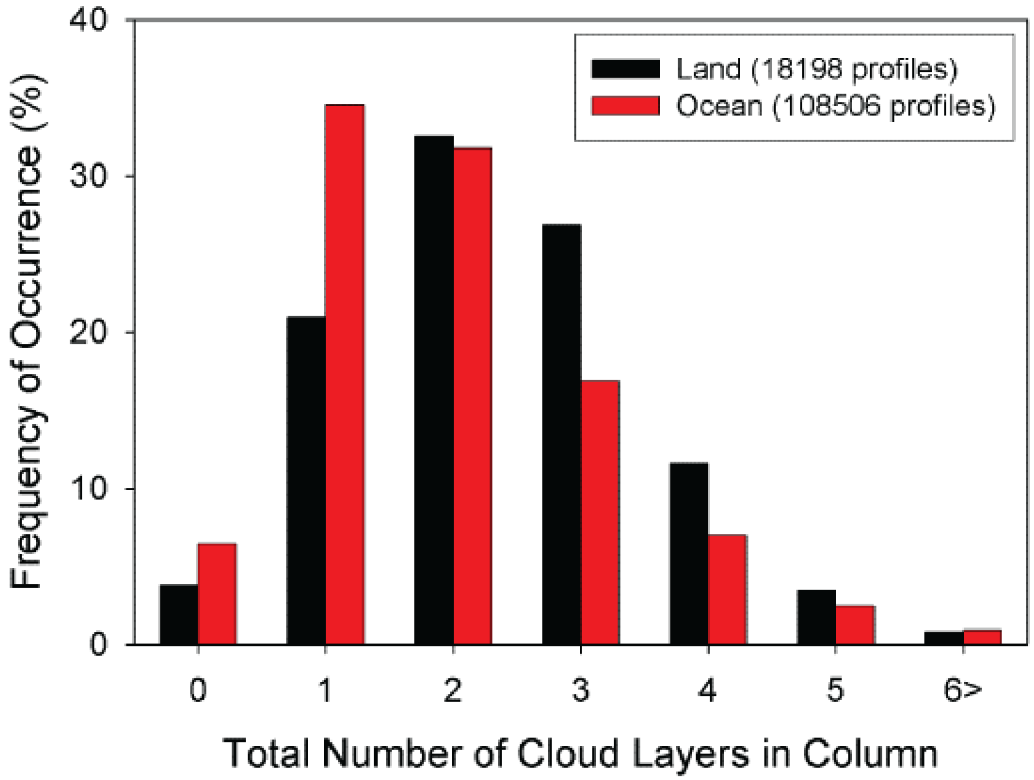

Figure 7. The frequency distribution of the total number of cloud layers over land (black) and over ocean (red). The average number of cloud layers for each region was 2.35 and 1.95 respectively. The number of profiles in each data set is shown in the legend.

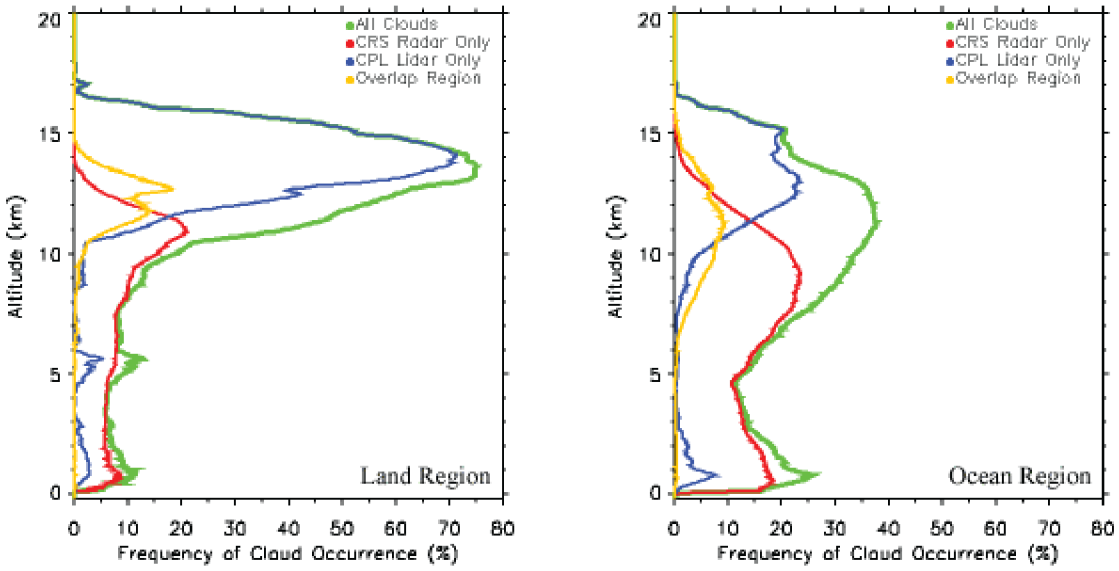

Figure 8. The vertical cloud distribution statistics over land (left) and over ocean (right) for the TC4 experiment. CPL sensed clouds only are shown in blue, clouds sensed by both instruments are in yellow, CRS sensed clouds only are in red, and total cloud volume from the merged CPL/CRS clouds is in green. Land profiles, which occurred much less frequently than water profiles, contained high-altitude clouds over 70% of the time.